

# Specialized stem cell niche enables repetitive renewal of alligator teeth

Ping Wu<sup>a</sup>, Xiaoshan Wu<sup>a,b</sup>, Ting-Xin Jiang<sup>a</sup>, Ruth M. Eley<sup>c</sup>, Bradley L. Temple<sup>d</sup>, Stephen J. Divers<sup>e</sup>, Travis C. Glenn<sup>d</sup>, Kuo Yuan<sup>f</sup>, Min-Huey Chen<sup>g,h</sup>, Randall B. Widelitz<sup>a</sup>, and Cheng-Ming Chuong<sup>a,h,i,1</sup>

<sup>a</sup>Department of Pathology, University of Southern California, Los Angeles, CA 90033; <sup>b</sup>Department of Oral and Maxillofacial Surgery, Xiangya Hospital, Central South University, Hunan 410008, China; <sup>c</sup>Louisiana Department of Wildlife and Fisheries, Rockefeller Wildlife Refuge, Grand Chenier, LA 70643; <sup>d</sup>Environmental Health Science and <sup>e</sup>Department of Small Animal Medicine and Surgery, University of Georgia, Athens, GA 30602; <sup>f</sup>Department of Dentistry and <sup>g</sup>Research Center for Wound Repair and Regeneration, National Cheng Kung University, Tainan City 70101, Taiwan; and <sup>h</sup>School of Dentistry and <sup>i</sup>Research Center for Developmental Biology and Regenerative Medicine, National Taiwan University, Taipei 10617, Taiwan

Edited by Edward M. De Robertis, Howard Hughes Medical Institute/University of California, Los Angeles, CA, and accepted by the Editorial Board March 28, 2013 (received for review July 31, 2012)

Reptiles and fish have robust regenerative powers for tooth renewal. However, extant mammals can either renew their teeth one time (diphyodont dentition) or not at all (monophyodont dentition). Humans replace their milk teeth with permanent teeth and then lose their ability for tooth renewal. Here, we study tooth renewal in a crocodilian model, the American alligator, which has well-organized teeth similar to mammals but can still undergo life-long renewal. Each alligator tooth is a complex family unit composed of the functional tooth, successional tooth, and dental lamina. Using multiple mitotic labeling, we map putative stem cells to the distal enlarged bulge of the dental lamina that contains quiescent odontogenic progenitors that can be activated during physiological exfoliation or artificial extraction. Tooth cycle initiation correlates with  $\beta$ -catenin activation and soluble frizzled-related protein 1 disappearance in the bulge. The dermal niche adjacent to the dental lamina dynamically expresses neural cell adhesion molecule, tenascin-C, and other molecules. Furthermore, in development, asymmetric  $\beta$ -catenin localization leads to the formation of a heterochronous and complex tooth family unit configuration. Understanding how these signaling molecules interact in tooth development in this model may help us to learn how to stimulate growth of adult teeth in mammals.

Wnt | placode | slow cycling | regeneration

Regenerative biology and medicine is emerging as a field with high potential for clinical applications. Nature is a rich resource from which to learn how to engineer stem cells for application to regenerative medicine, particularly for integumentary ectodermal organs such as hair, scales, nails, and teeth. These organs are at the interface between an organism and its external environment and therefore, face constant wear and tear (1). Animals have evolved successful regenerative mechanisms to accommodate renewal with minimal functional interruption (2). Feeding is critical for survival, but teeth unavoidably face frequent injury and loss. Most vertebrates replace teeth throughout their lives. Mouse incisor stem cells were found in the cervical loop (3). However, these stem cells are useful in sustaining continuous growth of incisors but not capable of generating replacement teeth. In the adult, stem cells from the dental pulp, periodontal ligament, dental follicle, and dental epithelium were identified in rodents and humans. They can differentiate into different cell types but cannot generate a whole tooth (4, 5). Our goal here is to identify stem cells that can be used as a resource for episodic tooth renewal.

Dental laminae, not present in mice, are considered to be the source of odontogenic stem cells for episodic tooth renewal (6–9). Zebrafish (teleosts) have a single row of pharyngeal teeth anchored by fusion to bone (ankylosis). These teeth are replaced continuously (polyphyodont) (10, 11). Reptiles such as snakes, geckos (8), and alligators (12, 13) can replace their teeth multiple times throughout their lives. In geckos (squamate reptiles), bromodeoxyuridine (BrdU) label was retained at the lingual portion of the dental lamina, representing putative odontogenic stem cells (14). In some mammals, such as young postnatal ferrets, teeth are

replaced from the dental lamina connected to the lingual side of the deciduous tooth (15). Human teeth are only replaced one time; however, a remnant of the dental lamina still exists (16) and may become activated later in life to form odontogenic tumors (17). Thus, much remains to be learned about the properties of the dental laminae.

We aspire to establish a model organism that has complex dental architecture and structures resembling those found in the mammal jaw but has the ability to replace its teeth multiple times. Although squamate (snake and lizard) teeth have recently been studied in detail (14), crocodilian teeth have a fundamentally different organization (Table S1). Squamates possess acrodont-pleurodont teeth (attached by connective filaments to the gum and maxillary/dental bones) (18), which differ from tooth attachment in mammals. Crocodilians have typical thecodont teeth, which show similar morphological characteristics as in mammalian teeth (they both are implanted in sockets of the maxillary/dental bones) (19). Crocodilians also have a secondary palate, like the palate found in mammals (20).

Adult alligators have 20 teeth in each quadrant arranged in a pseudoheterodont manner (21, 22) (Fig. 1A). Crocodilians frequently lose their teeth; each tooth is replaced about one time per year (12). Because crocodilians are long-lived, they may replace each tooth about 50 times (23). A small (replacement) tooth grows under each mature (functional) tooth, making a tooth family unit. The dental lamina splits off from the lingual side of the replacement tooth for subsequent tooth renewal (22, 24, 25). However, the molecular and cellular mechanisms regulating alligator tooth renewal remain elusive. Here, we apply stem cell biology techniques to revisit this classic model and explore how an alligator tooth family unit is built and maintained.

## Results

**Tooth Cycling in Alligators.** The 80 tooth family units present in embryonic and juvenile alligator jaws can be at different stages (phases) of development (13, 24, 25). Therefore, we documented the developmental stage of each tooth component within a tooth family unit using X-ray, microcomputed tomography (micro-CT), and serial paraffin sections. Although alligator teeth seem to cycle continuously, we defined three developmental phases for the tooth family units based on dental lamina morphology: (i) preinitiation stage, (ii) initiation stage, and (iii) growth stage (Fig. 1B and C and Table S2). In the preinitiation stage, the tooth family unit includes

Author contributions: P.W., R.B.W., and C.-M.C. designed research; P.W., X.W., T.-X.J., R.M.E., B.L.T., S.J.D., T.C.G., and K.Y. performed research; X.W., T.-X.J., R.M.E., B.L.T., S.J.D., T.C.G., and K.Y. contributed new reagents/analytic tools; P.W., R.B.W., and C.-M.C. analyzed data; and P.W., M.-H.C., R.B.W., and C.-M.C. wrote the paper.

The authors declare no conflict of interest.

This article is a PNAS Direct Submission. E.M.D.R. is a guest editor invited by the Editorial Board.

<sup>1</sup>To whom correspondence should be addressed. E-mail: cmchuong@usc.edu.

This article contains supporting information online at [www.pnas.org/lookup/suppl/doi:10.1073/pnas.1213202110/-DCSupplemental](http://www.pnas.org/lookup/suppl/doi:10.1073/pnas.1213202110/-DCSupplemental).

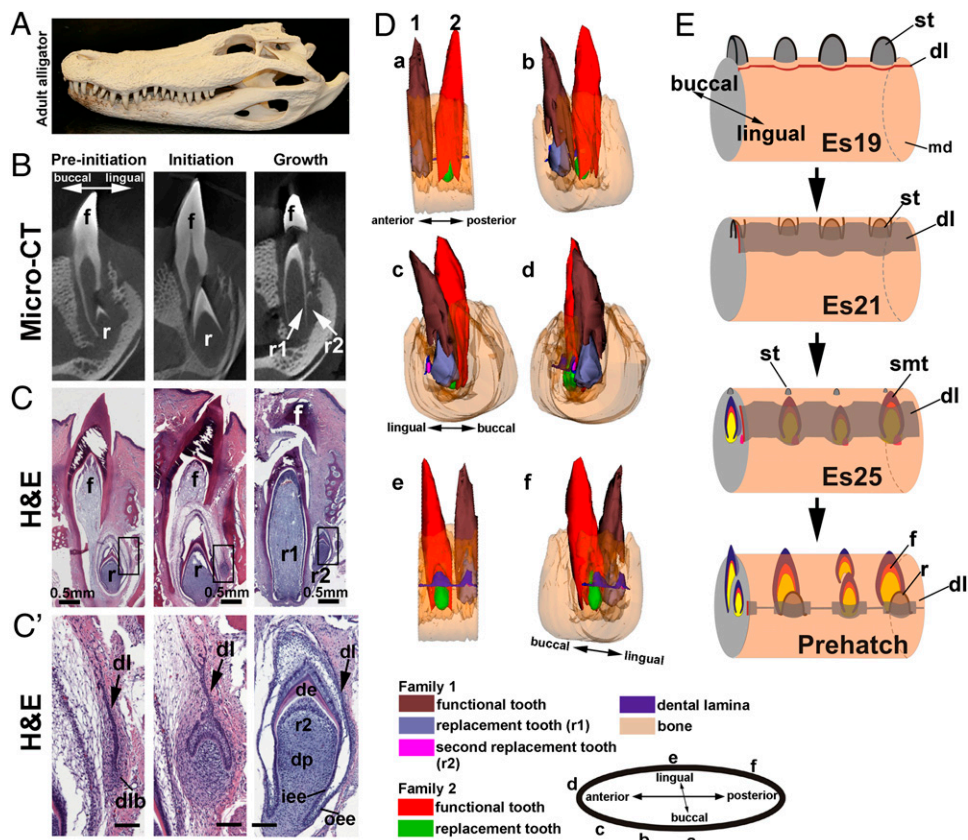


**Fig. 1.** Configuration of alligator tooth family units. (A) Adult alligator has 20 teeth in each quadrant. (B) Micro-CT and (C) H&E staining of paraffin sections from a 1-y-old alligator jaw. (C) Dental lamina, high magnification. (Left) Preinitiation stage. (Center) Initiation stage. (Right) Growth stage. Note that the dental laminae are not visible by micro-CT. The definition of the three stages is shown in Table S2. (D) 3D reconstruction of two tooth families from a 3-y-old alligator. Tooth family unit 1 is in growth stage, whereas family unit 2 is in preinitiation stage. The sections of H&E staining are shown in Fig. S1. (E) Diagram of tooth family unit development. The surface teeth at Es19 are invaginated and were resorbed. The dental lamina generated the submerged tooth, which becomes the future first functional tooth. The replacement tooth was generated by the dental lamina on the lingual side of the functional tooth. Before hatching, each tooth family unit developed at different times and represents different stages of family unit development. de, dentin; dl, dental lamina; dlb, dental lamina bulge; dp, dental papilla; f, functional tooth; iee, inner enamel epithelium; md, mandible; r, replacement tooth; r1, more mature replacement tooth in growth stage; r2, younger replacement tooth in growth stage; oee, outer enamel epithelium; st, surface tooth; smt, submerged tooth. (Scale bar: 100  $\mu\text{m}$ .)

a functional tooth (with the lingual root resorbed), a replacement tooth, and undifferentiated dental lamina (Fig. 1B and C, *Left*). In the initiation stage, the next replacement tooth starts to develop from the distal end of the dental lamina and forms a structure equivalent to the mouse cap-stage tooth germ (Fig. 1B and C, *Center*). When this tooth germ further develops to the bell stage, the tooth family unit is in the growth stage (Fig. 1B and C, *Right*). It includes a lost or nearly lost functional tooth, a first replacement tooth that is becoming a new functional tooth, and a second replacement tooth with a lingual dental lamina attached.

Interestingly, alligator dental laminae show additional structural specialization. To begin, juvenile and adult alligator dental laminae do not have a connection to the oral epithelium, which can be seen clearly in a 3D reconstruction of two adjacent tooth family units in a 3-y-old mandible (Fig. 1D). As shown by H&E staining in Fig. S1, family unit 1 is in early growth stage (Fig. S1A and A'), whereas family unit 2 is in preinitiation stage (Fig. S1C and C'). The tooth families are separated by dentary bone, but their dental laminae are connected with each other (Fig. S1B and B'). At the distal (aboral) end of the preinitiation-stage dental lamina, there is an enlarged cell cluster, which we term the dental lamina bulge (Fig. 1C', *Left* and Fig. S1C'). We hypothesize that, in alligators, odontogenic stem cells are concentrated in this dental lamina bulge. At the preinitiation stage, these cells have a latent status. During initiation stage, these cells are activated, and the bud will enlarge. Cells of the dental bud will proliferate, undergo morphogenesis to cap and bell stages, and differentiate into tooth organ components during the growth stage. To maintain renewal, when the outer enamel epithelium on the lingual side of the youngest replacement tooth splits to form an independent dental lamina, a stem cell niche needs to be retained to initiate the next tooth generation.

**Transient Amplifying Cells and Label-Retaining Cells in the Alligator Dental Lamina.** To examine the distribution of transient amplifying cells (TA cells) in the dental lamina at different stages, we

performed pulse BrdU labeling in juvenile alligators (Fig. 2A, *Left* and *SI Materials and Methods*); 3-h pulse labeling with BrdU shows that TA cells were enriched in initiation and growth stages (Fig. 2C and D) but sparse in the preinitiation stage (Fig. 2B and Fig. S2). Proliferation is low during the preinitiation stage, increases during initiation stage, and then decreases during the growth stage (Fig. 2B–D and K, blue bar). In comparison, at growth stage, the cervical loop of the replacement tooth has more proliferating cells than the dental lamina (Fig. 2D).

We used BrdU label retention to identify slow-cycling cells (potential stem cells) in the dental lamina of juvenile alligators (Fig. 2E–J and *SI Materials and Methods*). Alligators injected daily with BrdU for 1 wk to label proliferating cells (both fast- and slow-cycling cells) within this interval were euthanized after the 1-wk labeling period (no chase) or a 2- or 4-wk chase period (Fig. 2A, *Right*). After 1 wk of labeling, most of the nondifferentiated tooth epithelium cells (80%) in the replacement tooth were labeled with BrdU (Fig. 2G). However, only 10% of the dental laminae cells (at preinitiation and initiation stages) were BrdU-positive, which suggests that dental laminae cells are slow-cycling cells (Fig. 2E and F and Fig. S3A). After a 4-wk chase, the distribution of label-retaining cells (LRCs) was restricted to the distal end of the dental lamina at preinitiation stage and initiation stages (Fig. 2H and I). The LRCs were randomly distributed in the growth stage (Fig. 2J and L, red bar and Fig. S3B). Comparing the percentage of TA cells and LRCs during different cycle phases, we found that the dental lamina bulge has significantly more LRCs than TA cells in the preinitiation stage (Fig. 2K).

The number of BrdU-positive cells in the dental laminae (1-wk pulse) was compared with the number present after a 4-wk chase period. The dental laminae at preinitiation and initiation stage retained a similar number of LRCs as were present immediately after the 1-wk pulse (Fig. 2L, \*\*), whereas the replacement teeth retained few BrdU-positive cells at all stages (Fig. 2L).



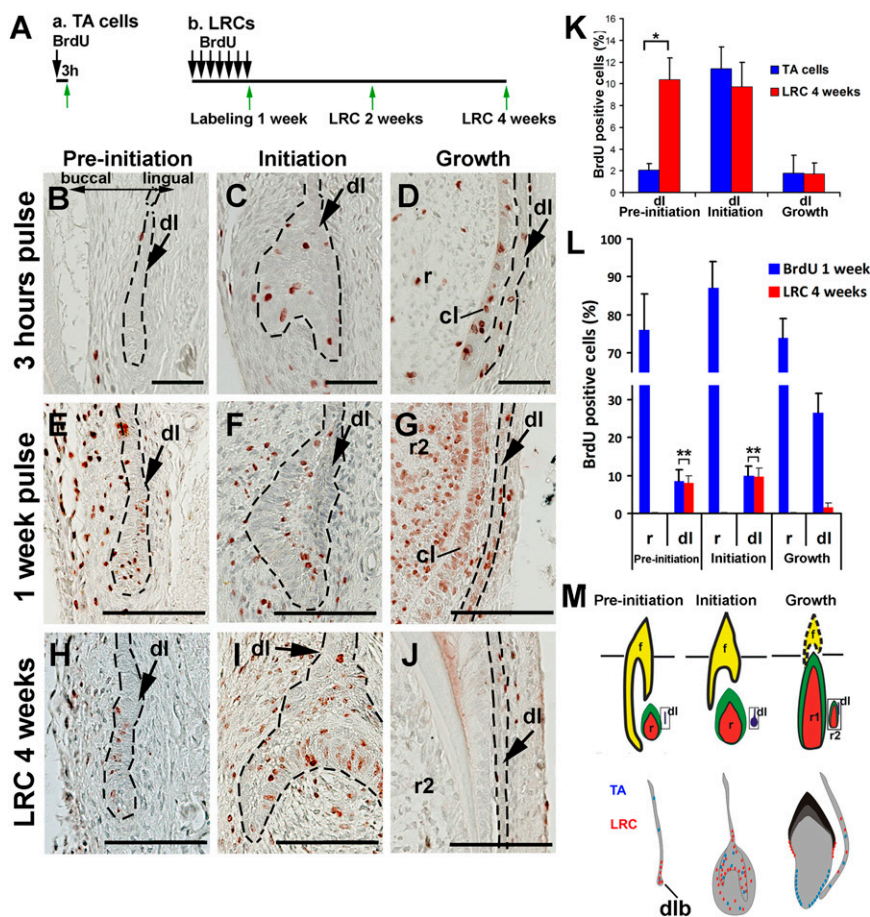


**Fig. 2.** LRC and TA cells in alligator tooth family units. (A) Experimental design of (Left) TA cells and (Right) LRC studies. (B–J) Localization of BrdU-positive cells after (B–D) 3 h pulse labeling, (E–G) 1-wk pulse-labeled TA cells, and (H–J) 4 wk chased LRCs in the dental laminae at different cycle stages. (Left) Preinitiation. (Center) Initiation. (Right) Growth. Detailed information is in Figs. S2 and S3. (K) Comparison of the percent TA cells and LRCs in the dental lamina at different cycle phases. (L) Comparison of BrdU-positive dental lamina cells resulting from a 1-wk BrdU pulse and a 4-wk chase in replacement tooth cervical loop epithelia and dental laminae at different cycle phases. (M) Diagram illustrates the distribution of TA cells (blue) and LRCs (red) at different cycle phases. cl, cervical loop; dl, dental lamina; dlb, dental lamina bulge; f, functional tooth; r, replacement tooth; r1, more mature replacement tooth in growth stage; r2, younger replacement tooth in growth stage. (Scale bar: 100  $\mu$ m.)

We conclude that the alligator dental laminae contain slow-cycling, putative stem cells. They were distributed in the distal end of the dental laminae at preinitiation stage. Some of these cells were retained during initiation and growth stages [Fig. 2M (LRCs are red)].

**Dynamic Change of TA Cells and LRCs During Physiological Exfoliation and Replacement of Alligator Teeth.** To examine alligator tooth replacement under physiological conditions, we tracked tooth exfoliation and renewal in juvenile alligators. First, we performed micro-CT on three juvenile alligators, representing developmental stages from hatchling to 1 y. Fig. 3A shows a micro-CT 3D reconstruction of the teeth and jaw of a 1-y-old individual to trace tooth family unit development. Tooth family units 4–7 on the right side of the mandible were highlighted. We used colors to indicate functional teeth (green) and replacement teeth (red). Some tooth family units, such as number 6, have already finished one cycle during this 1-y period.

Our model in Fig. 3B illustrates that, when the lingual side of the functional tooth is only partially resorbed, the dental lamina is attached intimately to the outer enamel epithelium of the newest forming replacement tooth during the preinitiation stage. When the replacement tooth grows to approximately one-half of its final size and the functional tooth is one-half to three-quarters resorbed, the dental lamina starts to differentiate to form a new tooth germ (initiation stage and then growth stage). We hypothesize that, in normal tooth replacement, preinitiation-stage stem cells in the dental laminae start to differentiate (initiation stage) (Fig. 3B, Lower Right) and grow further to become a new replacement tooth (growth stage) (Fig. 3B, Upper). Furthermore, when the new replacement tooth is mature enough, the lingual outer enamel epithelium will split and form a new preinitiation-stage dental lamina for the next cycle (Fig. 3B, Lower Left).

To examine the homeostasis of TA cells and LRCs during physiological tooth renewal, we performed Chlorodeoxyuridine (CldU) and Iododeoxyuridine (IdU) double labeling, which uses CldU to label LRCs and IdU to label TA cells (Fig. 3C and SI Materials and Methods). We compared 30 different tooth family units from the same individual and chose 6 of them to represent continuous cycling (Fig. 3D–I). The results are similar to the data obtained using BrdU to label TA cells and LRCs in different individuals (Fig. 2B–J). Here, we artificially separate the initiation stage into stages 1 and 2 and the growth stage into stages 1, 2, and 3. Increasing numeric value indicates increasing maturity. Progression through the tooth cycle shows that the TA cells (Fig. 3, blue staining and blue arrows) start to dramatically increase at early initiation stage (Fig. 3E, initiation 1) and peak at late initiation stage (Fig. 3F, initiation 2). When the tooth family unit starts to enter the growth stage (Fig. 3G and H, growth 1 and 2, respectively), proliferation in the dental lamina decreases, and finally, few positive TA cells could be detected at the end of growth stage (Fig. 3I, growth 3). However, a relatively similar number of LRCs (red arrow) is always present in the dental lamina at each developmental stage (Fig. 3D–I).

We conclude that, during tooth cycling, the number of TA cells peaked at late initiation stage, decreased at growth stage, and was further diminished at preinitiation stage, whereas the LRCs remained at similar levels during the whole cycle (Fig. 3J).

**Molecular Localization During Alligator Tooth Cycling.** Control of the Wntless/Int (Wnt)/ $\beta$ -catenin signaling pathway is essential for normal mammalian tooth development (26–30).  $\beta$ -Catenin is a multifunctional molecule that is involved in both cell–cell adhesion and signaling, and it has been implicated in the maintenance of stem cells.  $\beta$ -Catenin-overexpressing mice display multiple tiny teeth (27). Studies on severe hypodontia (missing

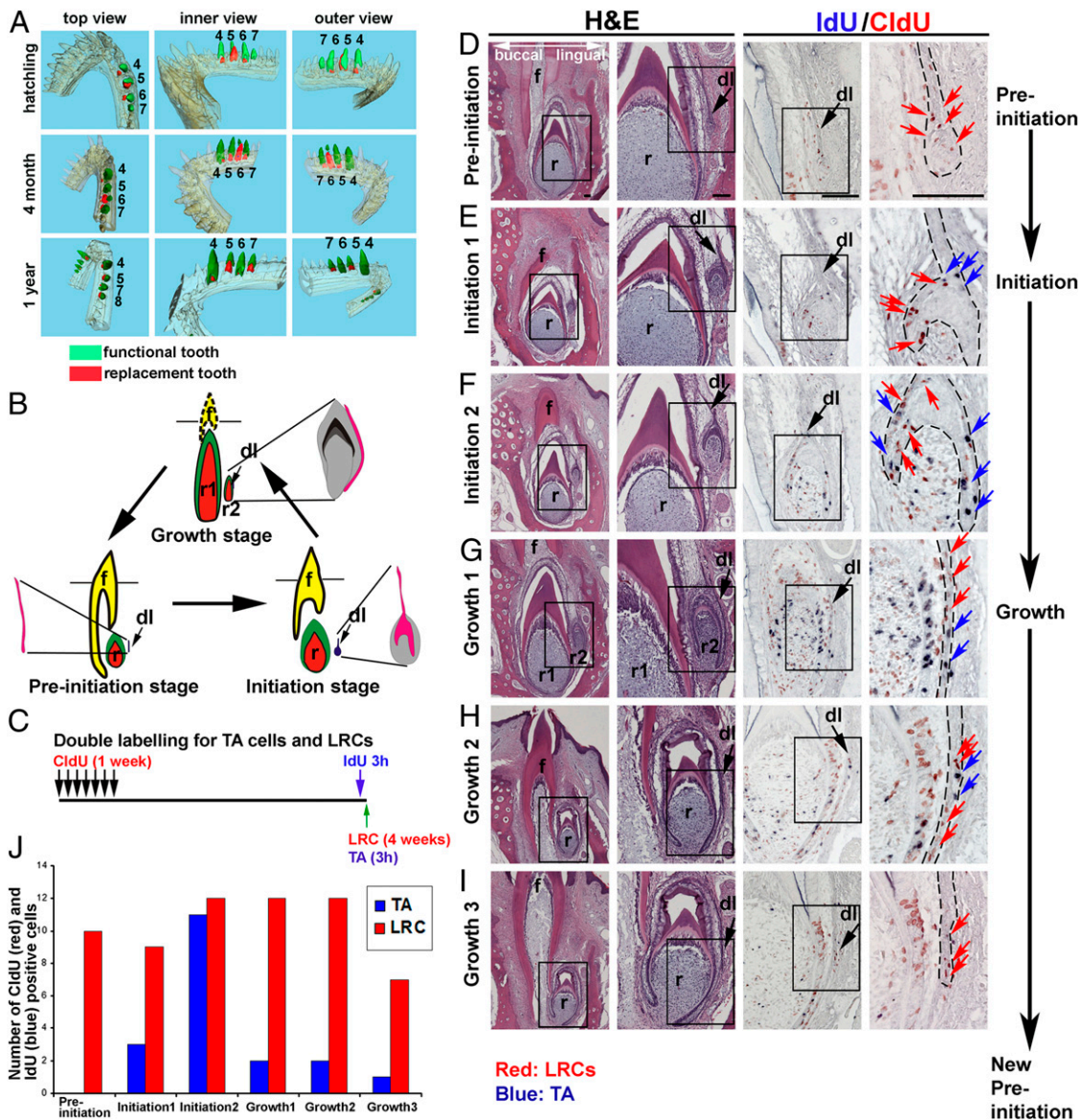


**Fig. 3.** Physiological exfoliation and dynamics of TA cells and LRCs by double labeling. (A) 3D reconstruction of micro-CT imaging was used to trace tooth family unit development from a hatching to a 1-y-old in an individual alligator. Tooth family units 4–7 in the right side of the mandible are highlighted with color (green for functional tooth and red for replacement tooth). Note that the dental laminae are not visible by micro-CT. (B) Tooth cycling stages. In normal exfoliation, the dental lamina at preinitiation stage starts to differentiate (*Lower Right*, initiation stage) and grow to be a new replacement tooth (*Upper*, growth stage). (C) Experimental design of double labeling. We used CldU (red) and IdU (blue) to label LRCs and TA cells, respectively. (D–I) Different stages of tooth family unit development. (D) Preinitiation stage. (E) Initiation stage. (F–I) Different growth stages showing how the replacement tooth matures. (Columns 1 and 2) H&E staining at different magnifications. (Columns 3 and 4) CldU and IdU double staining (red for CldU; blue for IdU) at different magnifications. Red arrows and blue arrows indicated LRCs and TA cells, respectively. dl, dental lamina; f, functional tooth; r, replacement tooth; r1, more mature replacement tooth in growth stage; r2, younger replacement tooth in growth stage. (Scale bar: 100  $\mu$ m.)

teeth) of permanent teeth in humans showed that Wnt signaling is required for both tooth initiation and replacement (31). Because alligators maintain their tooth renewal capabilities throughout life, these findings led us to explore whether  $\beta$ -catenin activity in the alligator dental laminae was critical to the tooth renewal process.

We used in situ hybridization and immunocytochemistry (*SI Materials and Methods*) to locate  $\beta$ -catenin mRNA transcripts and antigen within different stages of dental laminae in juvenile alligators. Probes were generated using polymerase chain reaction (PCR) primers listed in *Table S3*. At preinitiation stage,  $\beta$ -catenin transcripts and protein were focally located in the distal end of the dental lamina (Fig. 4A, *Top* and *B, Top*). In comparison, paired-like homeodomain transcription factor 2 (*Pitx2*), which is an epidermal marker expressed at different stages of tooth bud de-

velopment (32), was distributed throughout the dental lamina (Fig. S4A). In initiation stage, dental laminae in both  $\beta$ -catenin mRNA transcripts and antigen were diffusely detected, and  $\beta$ -catenin antigen was stronger on the buccal side (Fig. 4A, *Middle* and *B, Middle*). Both were present in the lingual outer enamel epithelium that was linked to the dental lamina at growth stage (Fig. 4A, *Bottom* and *B, Bottom*). Fluorescent immunostaining at the preinitiation stage showed that nuclear  $\beta$ -catenin-positive cells could be detected in the dental lamina bulge (Fig. S4D, arrows), but only cytoplasmic  $\beta$ -catenin was detected elsewhere (Fig. S4D). When the dental lamina is in initiation stage, cells with strong nuclear  $\beta$ -catenin staining could be detected in the inner enamel epithelium (Fig. S4E, arrows). At growth stage, only cytoplasmic  $\beta$ -catenin was found (Fig. S4F).



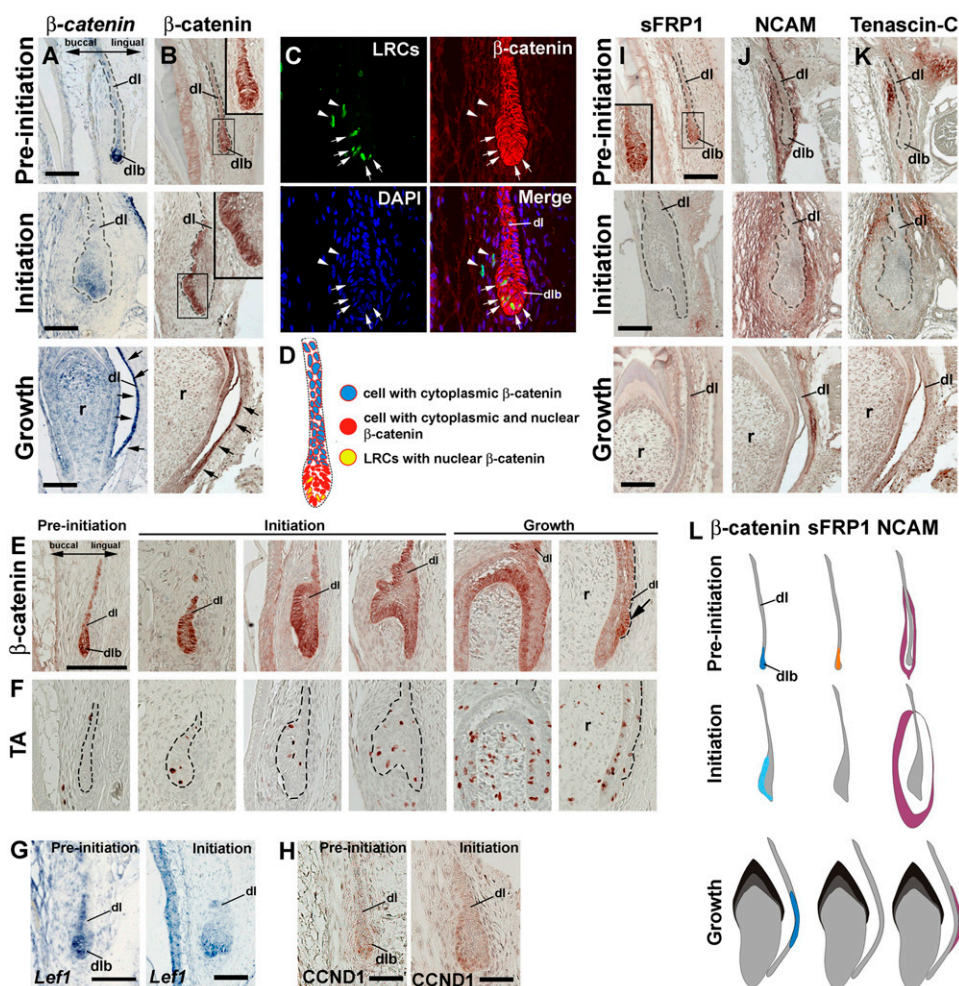


**Fig. 4.** Molecular localization in the dental laminae and their niche at different tooth cycling stages. (A, B, and I–K) Molecular localization at (Top) preinitiation, (Middle) initiation, and (Bottom) growth stages. (A)  $\beta$ -catenin transcripts. (B and I–K) Immunostaining for (B)  $\beta$ -catenin, (I) sFRP1, (J) NCAM, and (K) tenascin-C. (C) Triple staining for LRCs (CldU, green),  $\beta$ -catenin (red), and nuclei (DAPI, blue). White arrows indicate LRCs overlapping with nuclear  $\beta$ -catenin staining. White arrowheads indicate LRCs in the stroma. (D) Schematic drawing showing that LRCs overlap with nuclear  $\beta$ -catenin-positive cells in the dental lamina bulge. (E and F) Immunostaining for (E)  $\beta$ -catenin and (F) TA cells (3-h BrdU pulse) in dental laminae from different tooth unit stages of a newborn alligator jaw. Focal  $\beta$ -catenin distribution (arrow) in the budding dental lamina separating from a growth-stage replacement tooth indicates the start of a new cycle. (G) Localization of *Lef1* in (Left) preinitiation and (Right) initiation dental laminae. (H) Immunostaining of CCND1 in the dental lamina at (Left) preinitiation and (Right) initiation stages. (L) Diagram summarizing the distribution of  $\beta$ -catenin, sFRP1, and NCAM in the dental lamina niche. dl, dental lamina; dlb, dental lamina bulge; r, replacement tooth. (Scale bar: 100  $\mu$ m.)

To test whether nuclear  $\beta$ -catenin colocalizes with LRCs, we performed double fluorescent staining for  $\beta$ -catenin and LRCs (CldU chased for 4 wk) (Fig. 4C). LRCs were present in the dental lamina bulge and stroma. The LRCs overlapped with nuclear  $\beta$ -catenin-positive cells only in the dental lamina bulge (Fig. 4C, white arrows and D) and not in the stroma (Fig. 4C, white arrowheads).

In alligators, different tooth family units were at different phases (Fig. 4E). We used dental laminae from six different time points to show the process of dental lamina development;  $\beta$ -catenin antigen was diffusely distributed in the initiation stage (Fig. 4E) and became focally localized again when the dental lamina started to split from the replacement tooth (Fig. 4E, arrow). TA cells never overlapped with focally localized  $\beta$ -catenin at the stages that we studied (Fig. 4F).

To further test the involvement of the Wnt/ $\beta$ -catenin pathway in tooth renewal, we examined the location of Wnt pathway members. Soluble frizzled-related protein 1 (sFRP1), a Wnt pathway antagonist, was present in the preinitiation-stage dental lamina (Fig. 4I, Top) but was absent from the dental lamina at initiation and growth stages (Fig. 4I, Middle and Bottom). The disappearance of sFRP1 at initiation stage suggests that dental lamina initiation may require reduced Wnt inhibitor expression. The restricted nuclear  $\beta$ -catenin localization in the dental lamina bulge and the temporal-spatial dynamic expression of  $\beta$ -catenin and its members during tooth renewal suggest that  $\beta$ -catenin pathway is involved in regulating the quiescent and activated states of the tooth family.

Furthermore, we localized downstream Wnt signaling targets, such as lymphoid enhancer-binding factor 1 (*Lef1*) mRNA (Fig. 4G) and Cyclin D1 (CCND1) antigen (Fig. 4H) in the distal end of the dental lamina, at both preinitiation and initiation stages. These

data show that Wnt/ $\beta$ -catenin signaling is localized to the distal dental lamina bulge and supports their important involvement in tooth renewal.

We next examined the stromal niche surrounding the dental lamina and found neural cell adhesion molecule (NCAM), a cell adhesion molecule, localized in the stroma around the dental lamina at preinitiation stage (Fig. 4J, Top). When the dental lamina and surrounding mesenchyme proliferate in the initiation stage, the NCAM domain expanded (Fig. 4J, Middle). NCAM resumed its restricted pattern around the dental lamina during the growth stage (Fig. 4J, Bottom). Another cell adhesion molecule, tenascin-C, also was found surrounding the stroma with a pattern similar to NCAM but at a more peripheral region during preinitiation and initiation stages (Fig. 4K, Top and Middle). Tenascin-C antigen is absent during growth stage (Fig. 4K, Bottom). *Ods* (Osr2) and muscle segment homeobox 1 (*Msx1*) antagonize the patterning of tooth rows in mice (33). When we checked their mRNA distribution in alligator tooth family units, we found that both *Osr2* and *Msx1* were in the mesenchymal cells surrounding the dental laminae at preinitiation stage (Fig. S4B and C).

Thus, we found that  $\beta$ -catenin mRNA and antigen and sFRP1 antigen were present in the preinitiation-stage dental lamina bulge. *Msx1* and *Osr2* mRNA were in the surrounding stroma, and NCAM and tenascin-C antigen were positive in the surrounding regions (Fig. 4L). These data imply that the tooth renewal process may involve reestablishment of the stem cell niche.

**Precocious Replacement Tooth Initiation After Tooth Extraction in Juvenile Alligators.** The dynamic balance of tooth family unit components led us to hypothesize that extracting a functional

tooth might activate the differentiation of the preinitiation-stage dental lamina (Fig. 5I). Extracting the functional tooth ahead of its naturally programmed time point induced renewal. We performed a total of 20 tooth extractions in four individuals (1–3 y). After 8 wk, serial paraffin sections show that most of the manipulated tooth family units were in either the initiation or growth stage (18/20) (Fig. 5A). Only 10% (2/20) of the dental laminae were still in the preinitiation stage after extraction compared with 42% (21/50) during normal tooth renewal cycles. Dental laminae in extracted preinitiation-stage tooth families showed abnormal branching morphogenesis (Fig. 5B', blue arrow). One example showed abnormal crown invagination in the replacement tooth (Fig. 5B', black arrow) compared with an unextracted preinitiation-stage control (Fig. 5B). This result suggests that the dental lamina differentiates prematurely on extraction of the functional tooth.

To further test this hypothesis, we imaged four juvenile alligators (3 mo) with micro-CT to ascertain the tooth family unit stage and compare left–right symmetry. We chose corresponding preinitiation-stage tooth family units from the left and right sides of the 6-mo-old lower jaw for our regeneration studies. The functional tooth on the right side was extracted, and the corresponding left side was used as a control. CldU and IdU were used to label LRCs and TA cells, respectively (Fig. 5C). After 3 wk, we found that the dental lamina in the extracted tooth family unit was significantly increased in size (Fig. 5D') ( $n = 4/4$ ) compared with the unextracted control (Fig. 5D). A region of the activated

dental lamina showed focal  $\beta$ -catenin localization (Fig. 5E' compared with the control in Fig. 5E). The border of the dental lamina was expanded compared with the unextracted control as shown by NCAM staining (Fig. 5F' compared with the control in Fig. 5F). Quantification of TA cells and LRCs showed that, on removal of the functional tooth, the number of TA cells in the dental laminae was significantly increased, whereas the number of LRCs was similar to controls (Fig. 5G, G', and H).

Furthermore, we checked one preinitiation-stage tooth family (from a 3-y-old alligator) 2 wk after functional tooth extraction (Fig. S5A). Normally, initiation-stage dental laminae contained a single layer of nuclear  $\beta$ -catenin (Fig. S4E). After the functional tooth was removed, nuclear  $\beta$ -catenin localization expanded to multiple cell layers (Fig. S5B). *Left1* (Fig. S5C) and *CCND1* (Fig. S5D) were also found in this region. Overall, these ablation experiments suggest that proliferation and Wnt signaling in the dental lamina could be activated by premature removal of the functional tooth.

**Perturbation of the Wnt/ $\beta$ -Catenin Pathway During the Development of a Successional Tooth Family Unit in Alligators.** We used in vitro embryonic explant cultures to test the function of the Wnt/ $\beta$ -catenin pathway in the tooth renewal process, because it is not practical to do this experiment in postnatal alligators. Because alligator embryos show symmetric tooth development in the left and right sides, we cut the Es23 lower jaw into slices; we used the

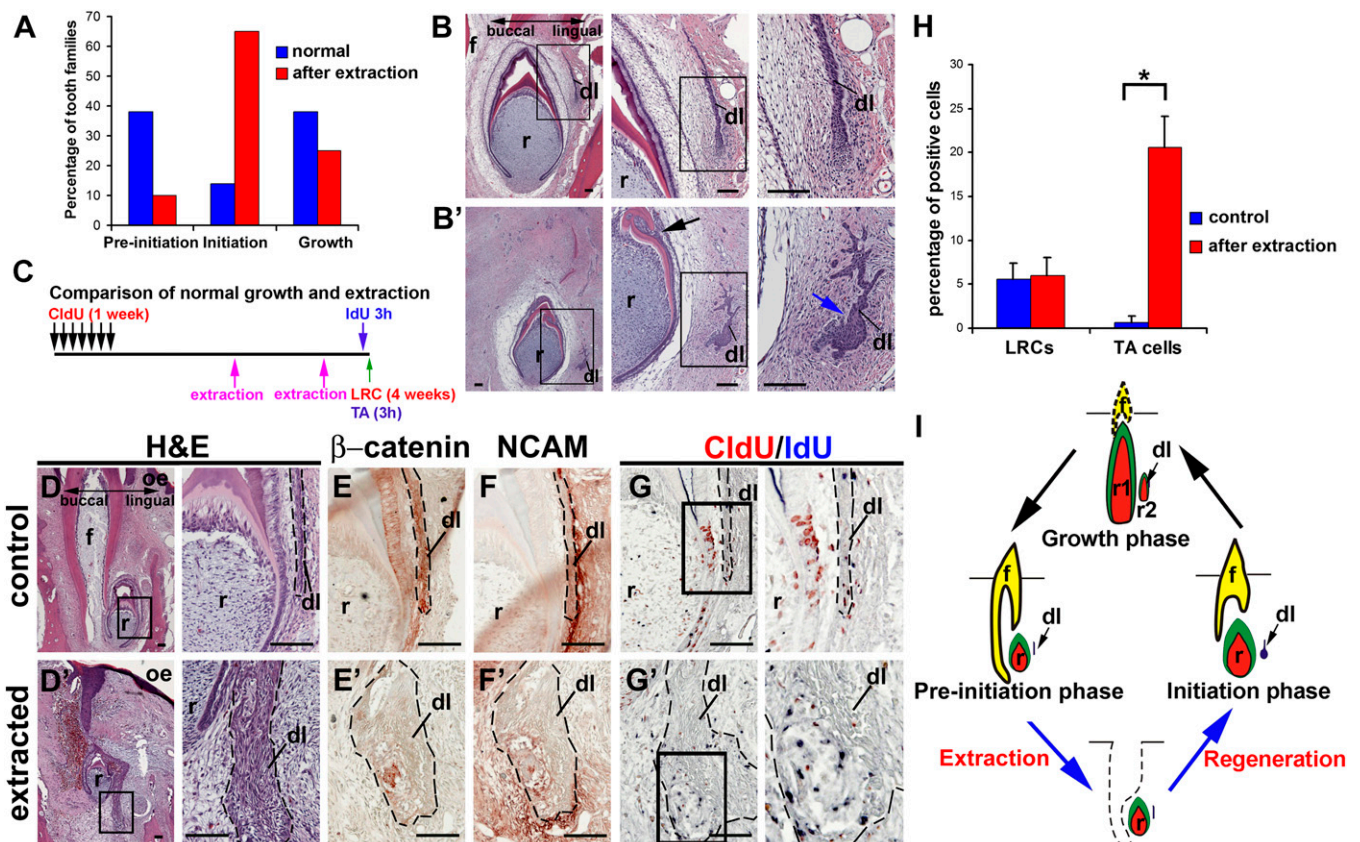


**Fig. 5.** Functional tooth removal accelerates dental lamina differentiation. (A) The percentage of tooth family units in preinitiation, initiation, and growth stages in control samples (blue bar) and after extraction (red bar). (B) Normal preinitiation stage dental lamina from a 3-y-old alligator. (B') Example of abnormal dental lamina morphogenesis after functional tooth removal. Black arrow indicates abnormal growth of a replacement tooth. Blue arrow indicates a branched dental lamina. (C) Strategy of LRC/TA cell labeling for the tooth extraction study. (D–G) The dental lamina accelerated differentiation after a functional tooth was extracted. (D–G) Unextracted control tooth family unit. (D'–G') Three weeks after extracting the functional tooth. (D and D') H&E staining. (E and E')  $\beta$ -Catenin localization. (F and F') NCAM distribution. (G and G') The distribution of LRCs (red) and TA cells (blue). (H) Statistics for the percentage of LRCs and TA cells in dental laminae between extracted (red bar) and unextracted (blue bar) tooth family units. (I) Diagram showing that removal of the functional tooth at preinitiation stage may accelerate the tooth renewal process. dl, dental lamina; f, functional tooth; oe, oral epithelium; r, replacement tooth. (Scale bar: 100  $\mu$ m.)



right side for experimentation, and we used the left side as a control. The slices were incubated with recombinant Wnt protein. Subsequent changes in  $\beta$ -catenin localization, proliferation, and apoptosis were surveyed.

First, we used recombinant Wnt3a protein to test the effect of increasing Wnt activity on tooth family unit formation (Fig. 6*A–E'*). Wnt3a treatment activated the distal region of the dental lamina (compare Fig. 6*A'* marked by the arrow with Fig. 6*A*) ( $n = 3/3$ ), mimicking changes observed during the initiation of tooth formation. The first step of dental lamina activation, whether by physiological initiation or extraction-induced initiation, was expansion at its base (Figs. 4*L* and 5*D'*). Therefore, we focused our analysis on the base of the dental lamina and compared the width of this region in Wnt3a-treated and control samples. This expansion is also shown in a 3D reconstruction (Fig. 6*E'* compared with Fig. 6*E*). The width of the enlarged region was measured from serial sections of treated (95.6- $\mu$ m) and control (56.8- $\mu$ m) samples.

We also found that  $\beta$ -catenin immunostaining increased in intensity in the Wnt3a-treated sample (Fig. 6*B'* compared with Fig. 6*B*). Cell proliferation detected by Proliferating Cell Nuclear Antigen (PCNA) staining was dramatically increased after Wnt3a treatment (87% positive in the dental lamina) (Fig. 6*C'*) compared with controls (36% positive) (Fig. 6*C*). We did not detect TUNEL-positive cells in either Wnt3a-treated samples (Fig. 6*D'*) or controls (Fig. 6*D*).

sFRP1 competes with membrane-bound frizzled receptors for binding to Wnts and leads to reductions in intracellular  $\beta$ -catenin (34). We used recombinant sFRP1 protein to test the effect of inhibiting  $\beta$ -catenin accumulation on establishing the tooth family unit. The tooth family units in experimental and control samples were both in a stage similar to the adult growth stage. Overexpressing sFRP1 led to a reduction in the size of the replacement tooth (Fig. 6*F'* compared with Fig. 6*F*) ( $n = 3/3$ ). The 3D reconstruction clearly shows that the replacement tooth had a dramatically reduced size (Fig. 6*J'* compared with Fig. 6*J*).  $\beta$ -Catenin immunostaining intensity decreased in the dental laminae of the treated sample (Fig. 6*G'* compared with Fig. 6*G*). We did not

detect differences in cell proliferation between the treated sample and control (Fig. 6*H'* compared with Fig. 6*H*); however, apoptotic cells were detected in the dental papilla (dp) of the sFRP1-treated replacement tooth (Fig. 6*I'*) but not in the control (Fig. 6*I*). The ectopic apoptotic cells in the dp may be responsible for reductions in the size of the replacement tooth. From these *in vitro* studies, we conclude that Wnt signaling can induce dental lamina proliferation and distal expansion, whereas Wnt inhibition can block the growth of replacement teeth by inducing dp cell apoptosis (Fig. 6*K*).

#### How Is the Formation of the Successional Tooth Family Unit Regulated During Embryonic Development?

To understand the molecular and cellular process involved, we examined how tooth family units form during embryonic development. Classical studies showed that the alligator tooth family units started to initiate at embryonic stage (Es)16 (13, 24, 25), when the first generation tooth (surface tooth) began to form. Surface teeth became resorbed and did not become functional. Around Es19–21, the dental lamina invaginated. The submerged tooth (the first future functional tooth) began to form at the distal end of the dental lamina at Es23 (Fig. S64). By Es25, the dental lamina separated from the submerged tooth and generated a new replacement tooth bud (Fig. S64). Embryonic alligator tooth family unit development is summarized in Fig. 1*E*. At prehatching stage, every tooth family unit consists of a functional tooth, a replacement tooth, and dental lamina (13, 24, 25) (Fig. 1*E*). The dental lamina in different tooth family units may be at different phases (preinitiation, initiation, or growth) (Fig. 1*E*).

We found that  $\beta$ -catenin transcripts were distributed asymmetrically in the tooth family unit in the pre-dental lamina at Es16, before dental lamina invagination, and in the dental lamina at Es18–20 after dental lamina invagination (Fig. 7*A* and *C*). At Es20,  $\beta$ -catenin was localized to the dental lamina at the lingual side of the surface teeth (Fig. 7*A* and *C*). At Es 21–24,  $\beta$ -catenin was still present in the dental lamina during submerged tooth formation and became focused at the distal end of the dental lamina (Fig. 7*C*). After the tooth family unit was fully established

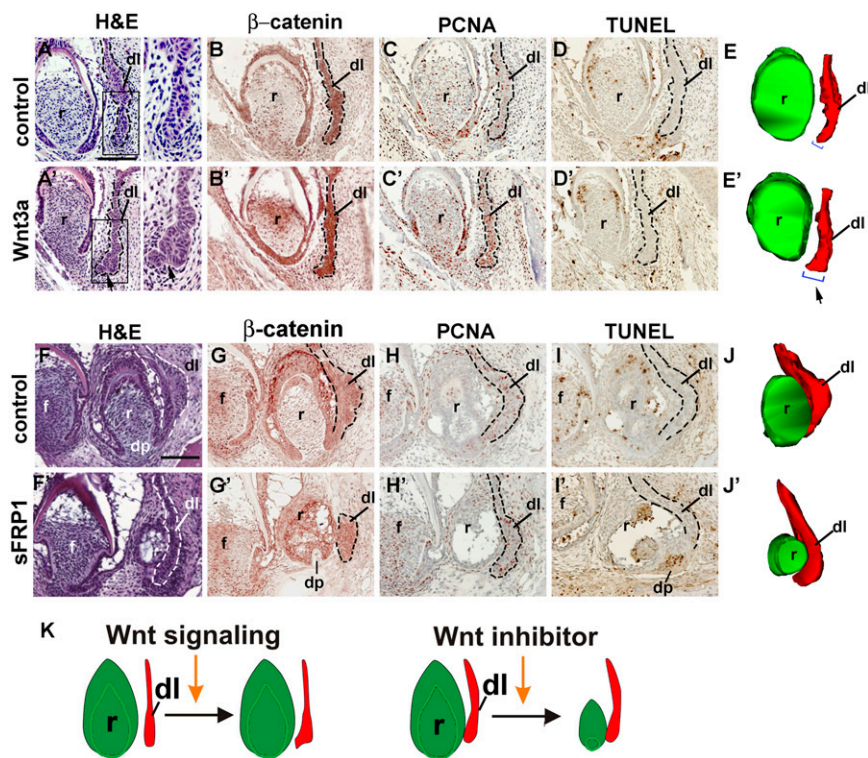


**Fig. 6.** Functional analysis in developing tooth family units. (A–E) The effect of Wnt3a treatment on tooth family unit development. (A–E) Control. (A'–E') Wnt3a-treated sample. (A and A') H&E staining. (B and B')  $\beta$ -Catenin immunostaining. (C and C') PCNA staining. (D and D') TUNEL staining. (E and E') 3D reconstruction. The bracket indicates the width of the distal end of the dental lamina. (F–J) The effect of sFRP1 treatment on tooth family unit development. (F–J) Control. (F'–J') sFRP1-treated sample. (F and F') H&E staining. (G and G')  $\beta$ -Catenin immunostaining. (H and H') PCNA staining. (I and I') TUNEL staining. (J and J') 3D reconstruction. (K) Schematic summary of functional analysis. dl, dental lamina; dp, dental papilla; f, functional tooth; r, replacement tooth. (Scale bar: 100  $\mu$ m.)

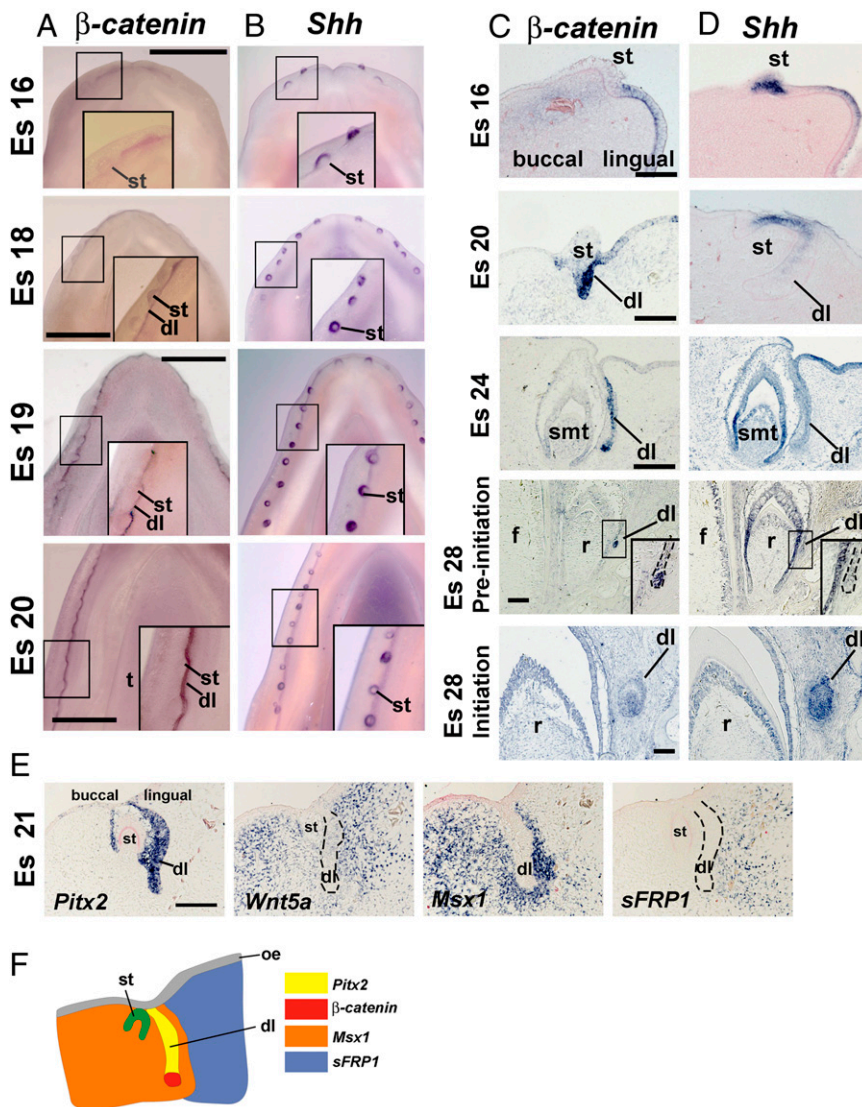


**Fig. 7.** Embryonic development of a tooth family unit. (A and B) Whole-mount in situ hybridization of (A)  $\beta$ -catenin and (B) *Shh* from stages 16 to 20.  $\beta$ -Catenin was found in the dental lamina, but *Shh* was present in the surface tooth. (C and D) Section in situ hybridization of (C)  $\beta$ -catenin and (D) *Shh* mRNA in the mandible from stage 16 to hatching alligators. At stage 28, in preinitiation stage, the distal part of the dental lamina expressed  $\beta$ -catenin but not *Shh* mRNA. When the dental lamina started to differentiate in the initiation stage,  $\beta$ -catenin became diffuse, but *Shh* levels were elevated and localized in the epithelium of the new tooth germ. (E) Localization of *Pitx2*, *Wnt5a*, *Msx1*, and *sFRP1* in stage 21 dental lamina. (F) Diagram of molecular distribution patterns at stage 21. *Pitx2* was distributed through the whole dental lamina, whereas  $\beta$ -catenin was localized in the distal end of the dental lamina. *Msx1* was found in both the stroma surrounding the dental lamina and the buccal side of the mesenchyme, whereas *sFRP1* was localized only in the lingual side of the mesenchyme. dl, dental lamina; f, functional tooth; r, replacement tooth; smt, submerged tooth; st, surface tooth; t, tongue. (Scale bars: A and B, 1 mm; C–E, 100  $\mu$ m.)

(stage 28),  $\beta$ -catenin transcripts displayed a similar pattern as the juvenile pattern (i.e., positive only in the distal part at preinitiation stage but diffuse during initiation stage). This unique pattern suggests that  $\beta$ -catenin may play important roles in tooth family unit formation and subsequent tooth renewal.

We then checked the distribution of  $\beta$ -catenin, tenascin-C, and amelogenin antigens in the developing tooth family unit from Es19 to -25 (Fig. S6).  $\beta$ -Catenin antigen was localized at the distal end of the dental lamina at Es21 and -24 before the submerged tooth and the replacement tooth germ formed (Fig. S6B, red arrows). Tenascin-C started to surround the distal end of the dental lamina from Es21 (Fig. S6C). Amelogenin, an enamel differentiation marker, was found in the ameloblasts in the distal regions of the replacement tooth from Es24, and staining became more intense at Es25 (Fig. S6D, blue arrow).

In comparison, sonic hedgehog (*Shh*) is present in the surface tooth and lingual oral epithelium at Es16–20 (Fig. 7B and D). At Es24, *Shh* transcripts were detected in the inner enamel epithelium of the bell-stage submerged tooth (Fig. 7D). Subsequently, it was found in the dental lamina at Es28 when the dental lamina started to differentiate to become a new tooth bud (Fig. 7D).

Because tooth differentiation occurred with a lingual to buccal orientation, we examined the distribution of known signaling molecules at Es21 before submerged teeth differentiated from the distal end of the dental lamina (Fig. 7E). We found that *Pitx2*

was distributed throughout the dental lamina and that *Wnt5a* was present in the mesenchyme surrounding the dental lamina. Neither *Pitx2* nor *Wnt5a* mRNAs showed buccal/lingual asymmetry. However, mesenchymal *Msx1* and *sFRP1* were differentially localized on the buccal and lingual sides, respectively. Although *Wnt5a* mRNA did not show a graded pattern, its inhibitor, *sFRP1*, was present on the lingual side, suggesting that an effective asymmetric buccal–lingual Wnt signaling distribution may play a role in establishing the observed differentiation from functional tooth to dental lamina within each tooth family unit (Fig. 7F).

## Discussion

**Special Features of Dental Lamina Organization in Alligator Tooth Family Units.** X-rays have been used to trace tooth family unit development (12, 13, 24, 25, 35). We observed dynamic tooth family development using micro-CT analysis and 3D reconstruction at different time points of tooth renewal (Figs. 1B and 3A). Our studies also used H&E staining to show histological changes, short- and long-term BrdU (and other thymidine analogs) labeling to study TA and stem cell distribution, and in situ hybridization/immunostaining to visualize the distribution of mRNA/antigen within the stem cell niche. Our study showed that a tooth family unit at each tooth position is composed of three components at different stages of development. The buccal functional tooth was the most



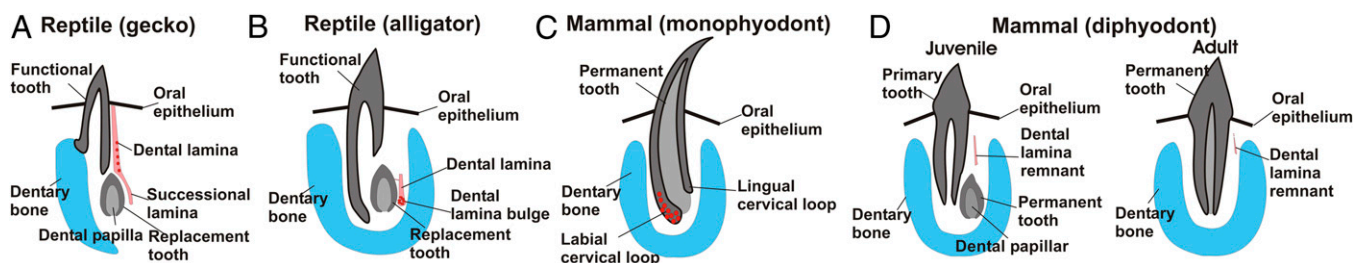


**Fig. 8.** Comparison of stem cell niches in adult gecko, alligator, and mammalian teeth. (A) Gecko's dental lamina is linked to the oral epithelium. LRCs (red dots) are diffusely distributed in the lingual portion of the dental lamina but excluded from their distal end (successional lamina) (14). (B) Adult alligator's dental lamina is not linked to the oral epithelium. LRCs are located in the distal tip of the dental lamina at preinitiation stage, which we name the dental lamina bulge. (C) Adult mice lack a dental lamina for tooth renewal. In incisors, stem cells for continual growth are located in the cervical loop (3). (D) Diphyodont mammals (including humans) have only two sets of dentition. After the crown of a permanent tooth formed, the dental lamina degenerated and became a remnant.

mature followed by the replacement (or successional) tooth and the lingual dental lamina. Tooth family units are arranged with proper configuration, and therefore, the transition from dislodgement to replacement can occur smoothly. The tooth family unit may be produced during embryonic development by forming molecular asymmetries, which split a single tooth primordium into three components. In this way, one tooth germ could become multiple entities, which are regulated by multiple signaling centers. However, the molecules secreted from the replacement tooth or by its local environment that trigger a preinitiation-stage dental lamina to differentiate remain elusive.

The dental lamina organization in alligators is more complex than the organization in other organisms that also form successional tooth family units. Fish dental laminae in each tooth family unit are interconnected (7). Gecko (Squamate) dental laminae are continuous and plate-like; they also connect with the oral epithelium (14). LRCs are located diffusely in the lingual portion of the dental laminae without clustering to the distal ends of the dental lamina (Fig. 8A) (14). In comparison, alligator dental laminae showed a more complex compartmentalization by forming a bulge at the distal tip of the dental lamina, where putative stem cells and  $\beta$ -catenin nuclear-positive cells reside (Figs. 4D and 8B and Table S1). We hypothesize that the emergence of the distal bulge in the dental lamina may help to pattern clustered stem cells during alligator tooth cycling that may maintain a niche for the persistence of tooth renewal for multiple generations. Furthermore, the dental laminae became disconnected from the oral epithelium, and tooth family units were separated from one another by bone. However, tooth family units were still interconnected by a string-like dental lamina (25) (Fig. 1D, Table S1, and Fig. S1B'). This interfamilial dental lamina also showed the presence of  $\beta$ -catenin (Fig. S1B').

**Cellular Dynamics and Tissue Interactions in Alligator Dental Lamina During Tooth Renewal Cycling.** We showed by BrdU label retention studies on juvenile alligators that cells present in dental laminae could retain label for at least 4 wk, suggesting that they are slow-cycling cells. These cells localized to the distal end of the dental laminae at preinitiation stage. Using CldU and IdU labeling, we also showed that LRCs were maintained throughout the tooth cycle, whereas the number of TA cells increased dramatically during early tooth initiation stage, decreased to the end of growth stage, and was greatly diminished during preinitiation stage. Extracting the functional teeth could activate these slow-cycling cells or the putative stem cells in the dental lamina and initiate the tooth cycle.

The importance of Wnt/ $\beta$ -catenin signaling in mouse tooth development has been reported (26–30). Here, we show that, in adult alligators, the distribution of  $\beta$ -catenin in the dental lamina bulge correlates with tooth renewal under physiological regenerative conditions. It is not practical to experiment on postnatal alligators, and a transgenic approach is not available; therefore, we used alligator mandible explant cultures for functional tests. In this system, overexpression of Wnt3a in the explant induced cell pro-

liferation in the dental lamina and led to bulge region expansion. However, addition of sFRP1, an antagonist of the Wnt/ $\beta$ -catenin pathway, led to reduced replacement tooth size. Because the technology is not available to transduce a target cell population, we cannot activate or suppress  $\beta$ -catenin specifically in putative stem cells. However, these results suggest that Wnt3a and sFRP1 may be involved in regulating dental lamina cycling by promoting or inhibiting the conversion of poised stem cells to TA cells, leading to the formation of the second replacement tooth.

With a clustered dental lamina bulge, we observed adjacent mesenchymal niches also changed dynamically at different cycling stages. For example, NCAM-positive mesenchyme surrounds the dental lamina and exhibited dynamic configurations during the tooth cycle (Fig. 4J). In this temporal and spatial framework, at Es21, *Wnt5a* was uniformly distributed in adjacent mesenchyme. The asymmetric distribution of the Wnt inhibitor, *sFRP1*, on the lingual side may inhibit Wnt signaling, leading to higher  $\beta$ -catenin activity on the buccal side. *Msx1*, important for terminal cell differentiation in the tooth (36), was found in the mesenchyme on the buccal side of the dental lamina (Fig. 7E). Together, these gene networks may help position the functional tooth on the buccal side and the dental lamina on the lingual side (Fig. 7F). It is possible that this configuration may keep stem cell activity balanced and capable of cyclic activation, similar to the molecular networks observed in hair bulge stem cells (37).

**Dental Laminae in Other Species and Implications for Regenerative Medicine.** In mice, which are monophodont, stem cells are located in the cervical loop of the mouse incisor (Fig. 8C) (3). Although incisors can grow long, mice cannot replace lost teeth. The dental lamina of diphyodont mammals (such as humans and pigs) is mostly degraded after generation of the replacement tooth (Fig. 8D). The process of dental lamina loss was studied, and laminin staining for the basement membrane was disrupted on the aboral side of the tooth. Most notable was the egress of keratinocytes from the pig dental lamina into the surrounding mesenchyme. Keratinocytes then went through an epithelial–mesenchymal transformation (38). Our studies on alligator tooth renewal suggest that Wnt signaling may be involved in maintaining specific segments of the dental lamina. The involvement of Wnt signaling will be explored further in future studies.

Our findings may also have implications in understanding human oral diseases. There are human syndromes in which supernumerary teeth form. Cleidocranial dysplasia syndrome is a human autosomal dominant disease likely to invoke runt-related transcription factor 2 (RUNX2) (39). Among other problems, these patients show multiple supernumerary teeth possibly derived from the dental epithelium of permanent teeth (40). Pathological examination revealed remnants of dental lamina around the extracted supernumerary teeth (41). Gardner syndrome is another disease in which supernumerary teeth form. Gardner syndrome is a variant of familial adenomatous polyposis, which is caused by loss-of-function germ-line mutations in the adenomatous

polyposis coli gene (42). Adenomatous polyposis coli inhibits Wnt/ $\beta$ -catenin signaling, disrupting its pivotal role in development and maintenance of homeostasis in adults (43, 44).

Based on our study, it may be possible to identify the regulatory network for tooth cycling. This knowledge will enable us to either arouse latent stem cells in the human dental lamina remnant to restart a normal renewal process in adults who have lost teeth or stop uncontrolled tooth generation in patients with supernumerary teeth.

## Materials and Methods

Fertilized alligator eggs were incubated at 30 °C and staged according to Ferguson (45). Embryos and hatchling to 3-y-old juvenile alligators were used for our studies. BrdU was used to measure cell proliferation. CldU and IdU were used to trace LRCs and TA cells, respectively (Fig. 5C). Jaws of live animals were imaged by Micro-CT. Slices of stage 23 alligator mandibles containing 1 family unit were grown on culture inserts in a Petri dish for 4 d

at 37 °C in culture media (46); 2  $\mu$ g Wnt3a or 10  $\mu$ g sFRP1 recombinant proteins were added to inhibit Wnt signaling. Dental lamina and replacement tooth sizes were compared between control and treated samples. Reconstruct software was used for 3D reconstruction (47). See *SI Materials and Methods* for experimental details.

**ACKNOWLEDGMENTS.** We thank the University of Southern California Molecular Imaging Core Facility for help in performing micro-CT analysis. We thank Chun-Chih Tseng for providing technical support. We appreciate the contributions of Jamie Williams, David Perpinan, and other University of Georgia Veterinary Medicine colleagues and students who assisted in performing the X-rays and helped with tooth extractions. We thank Drs. Harold Slavkin, Mark Ferguson, Irma Thesleff, and Joy Richman for their helpful comments. Confocal microscopy was performed by the Cell and Tissue Imaging Core of the University of Southern California Research Center for Liver Diseases (National Institutes of Health Grants P30 DK048522 and S10 RR022508). This research was supported by the National Institute of Arthritis and Musculoskeletal and Skin Diseases through Grants AR 42177, 60306 (to T.-X.J. and C.-M.C.), and 47364 (to C.-M.C.).

1. Chuong CM (1998) *Molecular Basis of Epithelial Appendage Morphogenesis*, ed Chuong CM (Landes Bioscience, Austin, TX), pp 3–14.
2. Wu P, et al. (2004) Evo-Devo of amniote integuments and appendages. *Int J Dev Biol* 48(2-3):249–270.
3. Harada H, et al. (1999) Localization of putative stem cells in dental epithelium and their association with Notch and FGF signaling. *J Cell Biol* 147(1):105–120.
4. Yen AH, Sharpe PT (2008) Stem cells and tooth tissue engineering. *Cell Tissue Res* 331(1):359–372.
5. Huang GT, Gronthos S, Shi S (2009) Mesenchymal stem cells derived from dental tissues vs. those from other sources: Their biology and role in regenerative medicine. *J Dent Res* 88(9):792–806.
6. Huysseune A, Thesleff I (2004) Continuous tooth replacement: The possible involvement of epithelial stem cells. *Bioessays* 26(6):665–671.
7. Smith MM, Fraser GJ, Mitsiadis TA (2009) Dental lamina as source of odontogenic stem cells: Evolutionary origins and developmental control of tooth generation in gnathostomes. *J Exp Zool B Mol Dev Evol* 312B(4):260–280.
8. Richman JM, Handrigan GR (2011) Reptilian tooth development. *Genesis* 49(4):247–260.
9. Moriyama K, Watanabe S, Iida M, Sahara N (2010) Plate-like permanent dental laminae of upper jaw dentition in adult gobioid fish, *Sicyopterus japonicus*. *Cell Tissue Res* 340(1):189–200.
10. Huysseune A, Van der heyden C, Sire JY (1998) Early development of the zebrafish (*Danio rerio*) pharyngeal dentition (Teleostei, Cyprinidae). *Anat Embryol (Berl)* 198(4):289–305.
11. Van der heyden C, Huysseune A, Sire JY (2000) Development and fine structure of pharyngeal replacement teeth in juvenile zebrafish (*Danio rerio*) (Teleostei, Cyprinidae). *Cell Tissue Res* 302(2):205–219.
12. Edmund AG (1962) Sequence and rate of tooth replacement in the crocodylia. *Contr Life Sci Div Roy Ont Mus* 56r:1–42.
13. Westergaard B, Ferguson MW (1990) Development of the dentition in Alligator mississippiensis: Upper jaw dental and craniofacial development in embryos, hatchlings, and young juveniles, with a comparison to lower jaw development. *Am J Anat* 187(4):393–421.
14. Handrigan GR, Leung KJ, Richman JM (2010) Identification of putative dental epithelial stem cells in a lizard with life-long tooth replacement. *Development* 137(21):3545–3549.
15. Järvinen E, Tummers M, Thesleff I (2009) The role of the dental lamina in mammalian tooth replacement. *J Exp Zool B Mol Dev Evol* 312B(4):281–291.
16. Philipsen HP, Reichart PA (2004) The development and fate of epithelial residues after completion of the human odontogenesis with special reference to the origins of epithelial odontogenic neoplasms, hamartomas and cysts. *Oral Biosci Med* 1:171–179.
17. Ide F, et al. (2007) Hamartomatous proliferations of odontogenic epithelium within the jaws: A potential histogenetic source of intraosseous epithelial odontogenic tumors. *J Oral Pathol Med* 36(4):229–235.
18. Schwenk K (2000) *Feeding: Form, Function and Evolution in Tetrapod Vertebrates* (Academic Press, San Diego), pp 1–564.
19. McIntosh JE, et al. (2002) Caiman periodontium as an intermediate between basal vertebrate ankylosis-type attachment and mammalian “true” periodontium. *Microsc Res Tech* 59(5):449–459.
20. Ferguson MW (1981) Developmental mechanisms in normal and abnormal palate formation with particular reference to the aetiology, pathogenesis and prevention of cleft palate. *Br J Orthod* 8(3):115–137.
21. Osborn JW (1975) Tooth replacement: Efficiency, patterns and evolution. *Evolution* 29(1):180–186.
22. Ferguson MW (1981) Review: The value of the American alligator (*Alligator mississippiensis*) as a model for research in craniofacial development. *J Craniofac Genet Dev Biol* 1(1):123–144.
23. Poole DFG (1961) Notes on tooth replacement in the Nile crocodile, *Crocodilus niloticus*. *Proc Zool Soc Lond* 136:131–160.
24. Westergaard B, Ferguson MWJ (1986) Development of the dentition in alligator mississippiensis: Early development of the lower jaw. *J Zool* 210(4):575–597.
25. Westergaard B, Ferguson MWJ (1987) Development of the dentition of alligator mississippiensis: Later development in the lower jaws of hatchlings and young juveniles. *J Zool* (1987) 212(2):191–222.
26. Sarkar L, Sharpe PT (1999) Expression of Wnt signalling pathway genes during tooth development. *Mech Dev* 85(1–2):197–200.
27. Järvinen E, et al. (2006) Continuous tooth generation in mouse is induced by activated epithelial Wnt/ $\beta$ -catenin signaling. *Proc Natl Acad Sci USA* 103(49):18627–18632.
28. Liu F, et al. (2008) Wnt/ $\beta$ -catenin signaling directs multiple stages of tooth morphogenesis. *Dev Biol* 313(1):210–224.
29. Chen J, Lan Y, Baek JA, Gao Y, Jiang R (2009) Wnt/ $\beta$ -catenin signaling plays an essential role in activation of odontogenic mesenchyme during early tooth development. *Dev Biol* 334(1):174–185.
30. Liu F, et al. (2010)  $\beta$ -Catenin initiates tooth neogenesis in adult rodent incisors. *J Dent Res* 89(9):909–914.
31. Lammi L, et al. (2004) Mutations in AXIN2 cause familial tooth agenesis and predispose to colorectal cancer. *Am J Hum Genet* 74(5):1043–1050.
32. Keränen SV, Kettunen P, Aberg T, Thesleff I, Jernvall J (1999) Gene expression patterns associated with suppression of odontogenesis in mouse and vole diastema regions. *Dev Genes Evol* 209(8):495–506.
33. Zhang Z, Lan Y, Chai Y, Jiang R (2009) Antagonistic actions of *Msx1* and *Osr2* pattern mammalian teeth into a single row. *Science* 323(5918):1232–1234.
34. Satoh W, Matsuyama M, Takemura H, Aizawa S, Shimono A (2008) *Sfrp1*, *Sfrp2*, and *Sfrp5* regulate the Wnt/ $\beta$ -catenin and the planar cell polarity pathways during early trunk formation in mouse. *Genesis* 46(2):92–103.
35. Shimada K, Sato I, Moriyama H (1992) Morphology of the tooth of the American alligator (*Alligator mississippiensis*): The fine structure and elemental analysis of the cementum. *J Morphol* 211(3):319–329.
36. Blin-Wakkach C, et al. (2001) Endogenous *Msx1* antisense transcript: In vivo and in vitro evidences, structure, and potential involvement in skeleton development in mammals. *Proc Natl Acad Sci USA* 98(13):7336–7341.
37. Kandyba E, et al. (2013) Competitive balance of intrabulge BMP/Wnt signaling reveals a robust gene network ruling stem cell homeostasis and cyclic activation. *Proc Natl Acad Sci USA* 110(4):1351–1356.
38. Buchtová M, Stembírek J, Glocová K, Matalová E, Tucker AS (2012) Early regression of the dental lamina underlies the development of diphyodont dentitions. *J Dent Res* 91(5):491–498.
39. Bufalino A, et al. (2012) Cleidocranial dysplasia: Oral features and genetic analysis of 11 patients. *Oral Dis* 18(2):184–190.
40. Jensen BL, Kreiborg S (1990) Development of the dentition in cleidocranial dysplasia. *J Oral Pathol Med* 19(2):89–93.
41. Lukinmaa PL, Jensen BL, Thesleff I, Andreasen JO, Kreiborg S (1995) Histological observations of teeth and periodontal tissues in cleidocranial dysplasia imply increased activity of odontogenic epithelium and abnormal bone remodeling. *J Craniofac Genet Dev Biol* 15(4):212–221.
42. Madani M, Madani F (2007) Gardner's syndrome presenting with dental complaints. *Arch Iran Med* 10(4):535–539.
43. Rajagopal J, et al. (2008) Wnt7b stimulates embryonic lung growth by coordinately increasing the replication of epithelium and mesenchyme. *Development* 135(9):1625–1634.
44. Clevers H, Nusse R (2012) Wnt/ $\beta$ -catenin signaling and disease. *Cell* 149(6):1192–1205.
45. Ferguson MW (1985) *Biology of the Reptilia*, eds Gans C, Billet F, Maderson PFA (Wiley, New York), pp 451–460.
46. Buchtová M, et al. (2008) Initiation and patterning of the snake dentition are dependent on Sonic hedgehog signaling. *Dev Biol* 319(1):132–145.
47. Fiala JC (2005) Reconstruct: A free editor for serial section microscopy. *J Microsc* 218 (Pt 1):52–61.